ISSN 0029-3865

CONSELHO NACIONAL DE DESENVOLVIMENTO CIENTÍFICO E TECNOLÓGICO - CNPq

CENTRO BRASILEIRO DE PESQUISAS FÍSICAS - CBPF

NOTAS DE FÍSICA

CBPF-NF-055/83

SMALL ANGLE X-RAY SCATTERING FROM HYDRATING TRICALCIUM SILICATE

by

D. Vollet, A. Craievich and M. Regourd

RIO DE JANEIRO

1983

SMALL ANGLE X-RAY SCATTERING FROM HYDRATING TRICALCIUM SILICATE

D. Vollet[1], A. Craievich[2] and M. Regourd[3]

[1]Instituto de Química - UNESP, Araraquara, Brasil

[2]Centro Brasileiro de Pesquisas Físicas e Instituto de Física e Química de São Carlos - USP, São Carlos, Brasil

[3]Centre d'Etudes et de Recherches de l'Industrie des Liants Hydrauliques, Paris, France

Abstract

The small-angle X-ray scattering technique was used to study the evolution of the structure of hydrated tricalcium silicate at room temperature. The changes in specific area of the associated porosity and the evolution of density fluctuations in the solid hydrated phase were deduced from the scattering data. A correlation of these variations with the hydration mechanism was tried.

Key words: Tricalcium silicate; SAXS; Hydration.

1 INTRODUCTION

The Portland cement is a polyphased building material containing mainly calcium silicates and aluminates. The tricalcium silicate, $Ca_3 SiO_5$, is the most important component and is responsible for the development of the early mechanical strength of mortars and concretes.

Many laboratory studies have concerned the hydration of C_3S (C=CaO, S=SiO_2, in the cement notation). The kinetics of the chemical reactions between C_3S and water are well represented by the evolution of the heat of hydration. The calorimetric curve is composed of (i) a sharp signal within the first minutes, (ii) a plateau almost athermal up to about two hours (called the dormant period or the induction period), (iii) a broad peak spanning several hours and corresponding to the setting and hardening.

The consolidation of the dispersed systems (C_3S and water) at the end of the dormant period is mainly due to the formation of a hydrated silicate called C-S-H (H=H_2O) and $Ca(OH)_2$ (1,2). The C-S-H, the composition of which depends on the fineness of C_3S, the water/solid ratio, the degree of hydration and the curing temperature (3), has typical structural features of a poorly crystallized material often considered a gel (4,5). This gel is constituted by coloidal crystallites. Fully hydrated C_3S pastes are porous with a discontinuous pore size distribution (4,6,7): fine pores of C-S-H (intragel pores) and capillary pores, or intergel-particule pores. The layered structure of C-S-H cristallites composed of CaO sheets, Si_2O_7 dimeric tetra-

hedra and H_2O molecules, is however nowhere nearly as well ordered as the layered structure of the montmorillonite or vermiculite.

The C-S-H microstructural heterogeneities (intra-gel) produce small-angle X-ray scattering (SAXS) [8,9]. Most of the inter-gel or capillary porosity are much coarser than the intra-gel porosity. It gives a minor contribution to SAXS in the experimentally accesible angular domain. Winslow and Diamond [8] determined the specific surfaces of hardened portland cement samples. Their results are in general agreement with those obtained by water vapor adsorption in fully hydrated cement pastes [10]. Winslow and Diamond [8] and Lachaud [9] reported SAXS for a normal cement sample that reveals a positive deviation from Porod's law [11]. Such deviation is expected in the case of existence of one-dimensional density fluctuations in the system [11].

This paper is devoted to the measurement of the time evolution of SAXS from hydrating C_3S, in order to contribute to the characterization of its structure transformations.

2 SAMPLES AND METHODS

Pure synthetic and microgranulated C_3S was mixed with distilled water in a water/solid weight ratio of 0.5 and moulded into a sealed support to avoid water evaporation during the SAXS measurements. The experiments were carried out at room temperature (about 22^0C), using Cu K α radiation with a wavelength $\lambda = 0.154nM$. A beam having an approximately "linear and infi-

nite" cross-section [12] was employed.

The collection of the X-ray scattering data was done by using a standard small-angle goniometer and scintillation counter. The intensities were measured during a counting time of 180 sec at every scattering angle along the hydration process. The minimum and maximum scattering angles were 0.2 and 2.2^0, respectively, and the step angle $\Delta\varepsilon = 0.1^0$. The elapsed scanning time for the whole angular domain was about one hour. These measurements provided a number of plots of the scattering intensity as a function of the hydration time, I(t), for the different scattering angles. From this set of I(t) curves, the scattering intensity as a function of the scattering angle, $I(\varepsilon)$, were derived for different hydration times. The scattering intensities were determined in relative units.

The SAXS data were analysed, mainly, using Porod's law that holds for "two electronic density" systems composed of spheroidal particles, or voids (neither plate nor needle-like particles). Under the experimental conditions of "linear and infinite" collimation, the asymptotic dependence of the scattering intensity j(h), is given by [12]:

$$j(s \to \infty) = \frac{(\Delta\rho)^2 S}{16\pi^2 s^3} \qquad (1)$$

where $\Delta\rho$ is the difference in electron density between "particles" and matrix, S is the interphase area and s is the modulus of the scattering vector. S is related to the scattering angle ε by $s = 2\sin(\varepsilon/2)/\lambda$ ($s = \varepsilon/\lambda$ for small scattering angles). If the SAXS intensity is determined in absolute units and the electron density difference $\Delta\rho$ is known, the interface area S

can be derived from Porod's law. Often the intensity is not determined in an absolute scale. In this case the following expression is used [11]:

$$\frac{\lim 16\pi^2 j(s)s^3}{2\pi\int_0^\infty s\, j(s)ds} = \frac{S}{c(1-c)V} \qquad (2)$$

where S/V is the interface area per unit volume of the sample and c is the volume fraction of one of the phases. Equation (2) furnishes the specific surface provided c is known.

Systematic deviations from Porod's law can occur when there are electronic density fluctuations in the phases (positive deviation) or when the interphase is not well defined (negative deviation) [11]. In the case of positive deviation, when there is no correlation between the fluctuations in the matrix and its boundaries, the corresponding intensity component and the scattering of the ideal "two density system" are simply additive.

When a porous system has a matrix with layered structure a positive deviation from Porod's law is often experimentally observed. This deviation is related to fluctuations in the interlayer distances [11]. The asymptotic SAXS intensity is given by

$$j(s) = \frac{(\Delta\rho)^2 S}{16\pi^2 s^3} + \frac{V_1 \rho_1 \tau [F\ell]_1}{2s} \qquad (3)$$

where V_1 and ρ_1 are the volume and electron density of the matrix, respectively, τ is the surface density of electrons in the two-dimensional layers and $[F\ell]_1$ is the one-dimensional

fluctuation magnitude which is related to the fluctuations in the distances between layers, Δa_3, and in their diameters, ΔL, by [11]:

$$[F\ell]_1 = \frac{\langle \Delta^2 a_3 \rangle}{\langle a_3 \rangle^2} + \frac{\langle \Delta^2 L \rangle}{\langle L \rangle^2} \qquad (4)$$

where the symbol < > indicates average values.

Experimental SAXS results are usually represented by $j(s)s^3$ versus s^2 plots. If the SAXS intensity verifies equation 3, a linear behavior should be observed:

$$j(s)\, s^3 = a + b\, s^2 \qquad (5)$$

where $a = (\Delta\rho)^2\, S/16\pi^2$ and $b = V_1 \rho_1 \tau [F\ell]_1/2$. The extrapolation towards $s = 0$ of $j(s)s^3$ yields the value of the a parameter, which is related to the porosity interface area. The slope b of the straight line provides the fluctuation term which is associated with electron density fluctuations in the matrix. We will call a and b as "surface parameter" and "fluctuation parameter", respectively. Previous SAXS results on cements [8][9] showed the asymptotic behavior predicted by equation 5.

The lowest angle side of SAXS curves is usually analysed by means of Guinier's law. It holds for two density systems composed by isolated particles, or voids, having a narrow size distribution. In this case the SAXS intensity function is a gaussian and, therefore, the plots of $\ell og\, j(s)$ versus s^2 exhibit a linear behavior [13].

3 EXPERIMENTAL RESULTS AND DISCUSSION

The SAXS intensity functions, j(s) corresponding to the different hydration times, were experimentally obtained in relative units as described in the precedent section. The experimental intensity, after substracting the parasitic scattering, are plotted in Fig. 1 in $\log j(s)$ versus s^2 scale. The different plots corresponding to all hydration times show a clear positive curvature. This feature is due to the existence of a wide distribution of pore sizes. Thus, Guinier's law is not useful in this case to characterize the time evolution of the porosity.

The evolutions of the scattered X-ray intensity as a function of time, for various s values, are plotted in Fig. 2. The SAXS intensities I(t) exhibit an almost constant value up to about t= 5 hours, a rapid increase from 5 to approximately 25 hours and a slow increase for t > 25 hours.

A plot of $j(s)s^3$ versus s^2 of a C_3S sample in advanced stages of hydration is given in Fig. 3. It clearly shows the linear behavior which is expected from a "two density" system with one-dimensional density fluctuations in one of the phases (equations 5). This scattering is produced by the imperfect and porous C-H-S gel. The equivalent plots for the C_3S system, in earlier stages of hydration, also show a linear behavior as it can be seen in Fig. 4.

From the plots of Fig. 4 the surface parameter, a, and the fluctuation parameter, b, were determined for every hydration time. Their values are both plotted in Fig. 5. The sur-

face and fluctuation parameters have a correlated increase with time up to approximately 25 hours as it can be seen in Fig. 5. The equivalent plots corresponding to more advanced stages of hydration are shown in Fig. 6. We can see that the fluctuation parameter becomes constant for long hydration times but the surface parameter still increases. Nevertheless its variation is much slower than in early stages.

The s-dependence of the SAXS intensity given by equation 3, which was found in our experimental study, can be explained on the basis of the structure model of Feldman and Sereda [8] for hydrated C_3S. One of the phases of the Porod "two density system" in this model is constituted by the inter-crystallite pores and, the other, by the layered and poorly crystallized C_3S hydrated matrix. Between the layers there is, in fact, thin water layers. This kind of very imperfect stacking of hydrated C_3S layers leads to a system with essentially one-dimensional fluctuations in electronic density.

The density fluctuations found in C-S-H are similar to those reported in other layered structures like glassy carbon [12] which consists of randomly stacked graphite-like layers. Daimon et al. [3] found only diffused (hk0) X-ray reflections in diffraction patterns of C-S-H, revealing the existence of a disordered stacking of layers.

Since the intensities were measured in relative units, we also determined from equation 5 the time evolution of the surface parameter in relative units. Assuming a constant value of $(\Delta\rho)^2$ during hydration, the experimental surface parameter provides the time evolution of the porosity interface

area in relative units. The increase of the interface area may be mainly due, to the increase of the volume fraction of the gel matrix. This statement seems to be corroborated by the correlated variation of the fluctuation parameter. As a matter of fact the increase of gel volume, V_1, also explain the correlated increase of the fluctuation parameter during the first 25 hours of hydration (equation 3).

It should be mentioned that we have not be able to determine the actual interface area of the pores by using equation 2 because the volume fraction of porosity is not known. The method which was used by Winslow and Diamond[8] of weighting the removed water in a drying process cannot be applied to this kind of kinetical study of hydration.

The approximate constant value of the fluctuation parameter at advanced hydration stages (Fig. 6) may be due to a much slower formation of C-S-H gel. This would mean that the volume fraction, V_1, of gel and the interphase area of the intra-gel pores, S, are essentially time independent. We therefore assigned the remaining slow increase of the "surface parameter" to a slow variation of the electron density difference, $\Delta\rho$, between pores and gel matrix. The assumption of nearly time independent $\Delta\rho$ in earlier stages would no longer be valid at advanced stages of hydration. Since a and b are proportional to $(\Delta\rho)^2$ S and $V_1\rho_1$ $[F\ell]_1$, respectively, a variation of $\Delta\rho$ due to a decrease of the electron density of the pores would account for, both, the constancy of the fluctuation parameter and the increase of the surface parameter. Being the pores filled in the first stages with water, the experimental results for long times

may be explained as a consequence of a slow removal of free water from the intra-gel pores.

CONCLUSIONS

The variations of the surface and fluctuation parameters (Fig. 5 and 6) determined from our experimental SAXS results define three stages of C_3S hydration.

The first stage is characterized by a nearly constant interface area and a negligible fluctuation parameter. This early stage corresponds to the athermal plateau of the calorimetric curves (dormant period). The second stage is associated with the rapid increase of the surface and fluctuation parameters. This increase is correlated with the broad peak of the calorimetric curves (setting and hardening). The third stage, without important thermal effects, is characterized by an increase of the surface parameter and constancy of the fluctuation parameter.

The low and almost constant value of the surface parameter during the first stage may be due to the contribution to x-ray scattering from the interfaces between C_3S particles and water. The formation of a submicroscopic porous structure within an imperfect gel matrix is responsible for the increase in SAXS intensity during the second stage. The correlation between the surface and fluctuation parameters is a consequence of the increase in volume fraction of porous and poorly crystallized C-H-S gel. The slower process of the third stage seems to be mainly related to the slow removal of free-water from the intra-gel pores.

The SAXS technique allowed us to follow indirectly the hydration process of C_3S by studying the associated porosity and density fluctuations which develop during the C-H-S gel formation. SAXS may also be useful to study the first minutes of hydration (at which a sharp calorimetric signal is observed), provided a more intense beam, than that furnished by conventional generators, is used. Synchroton radiation and position sensitive detectors seem to be useful for studying the very early stages since they permit to reduce drastically the counting times of SAXS measurements. This will be done later on.

REFERENCES

1. P.A. Kittl, "Estado atual do mecanismo de hidratação do cimento", Revista Brasileira de Tecnologia, 8, 57-62 (1977)

2. M.E. Tadros, J. Skalny, and R.S. Kalyoncu, "Early hydration of tricalcium silicate", J. Am. Ceram. Soc., 59 [7-8], 344--347 (1976)

3. A. Bentur and R.L. Berger, "Chemical composition of C-S-H gel formed in the hydration of calcium silicate pastes", J. Am. Ceram. Soc., 62 [3-4], 117-120 (1978)

4. M. Daimon, S.A. Abo-El-Enein, G. Hosaka, S. Goto, and R. Kondo, "Pore structure of calcium silicate in hydrated tricalcium silicate", J. Am. Ceram. Soc., 60 [3-4], 110-114 (1977)

5. P.A. Slegers, M. Genet, A.J. Leonard, and J.J. Fripiat,"Structural transformation of tricalcium silicate during hydration", J. Appl. Cryst., 10, 270-276 (1977)

6. S. Brunauer, J. Skalny, and I. Odler, P.P. 3-26 (1973) in Pore Structure and Properties of Materials, Proceedings of the International Symposium of RILEM-IUPAC, Prague, 1973, Part I, C. Academia Prague (1973)

7. R.L. Feldman, pp.53-66 in Proceedings of the 5thInternational Symposium on the Chemistry of Cement, Vol. III, The Cement Association of Japan, Tokyo (1969)

8. D.N. Winslow and S. Diamond, "Specific surface of hardened portland cement paste as determined by small angle X-ray scattering", J. Am. Ceram. Soc., 57 [5], 193-197 (1974)

9. R. Lachaud, "Possibilités de la diffusion centrale dans l'examen d'états alterés du ciment", Cement and Concrete Research, 6 [4], 571-581 (1976)

10. R.Sh. Mikhail, D.H. Turk, and S. Brunauer, "Dimensions of the average pore, the number of pores, and the surface area of hardened portland cement paste", Cement and Concrete Research, 5 [5], 433-442 (1975)

11. W. Ruland, "Small-angle scattering of two phase systems: determination and significance of systematic deviation from Porod's law", J. Appl. Cryst., 4, 70-73 (1971)

12. V. Luzzatti, "Interpretation des mesures absolues de diffusion centrale des rayons X en collimation ponctuelle ou lineaire: solutions de particules globulaires et de bâtonnets", Acta Cryst., 13, 939-945 (1960)

13. A. Guinier and G. Fournet, "Small Angle Scattering of X-rays", J. Wiley (1955)

14. A. Craievich and E. Dujovny, "Submicroscopic voids in glassy carbon", J. Mat. Sci., 8, 1165-1170 (1973)

FIGURE CAPTIONS

Figure 1: Guiner's plots for different hydration times.

Figure 2: Scattered intensity versus time of hydration for fixed s values.

Figure 3: Porod's plot for long time of hydration.

Figure 4: Porod's plots along hydration for increasing times [h]:

● 5, ◘ 7.5, ♦ 10, ◊ 12.5, ▲ 15, ▲ 17.5, ▼ 20, ▽ 22.5, ■ 25, ◘ 30, ◘ 47.5, ◆ 68, ■ 103.5, x 168.

Figure 5: Surface (a) and fluctuation (b) parameters during hydration.

Figure 6: Surface (a) and fluctuation (b) parameters for advanced stages of hydration.

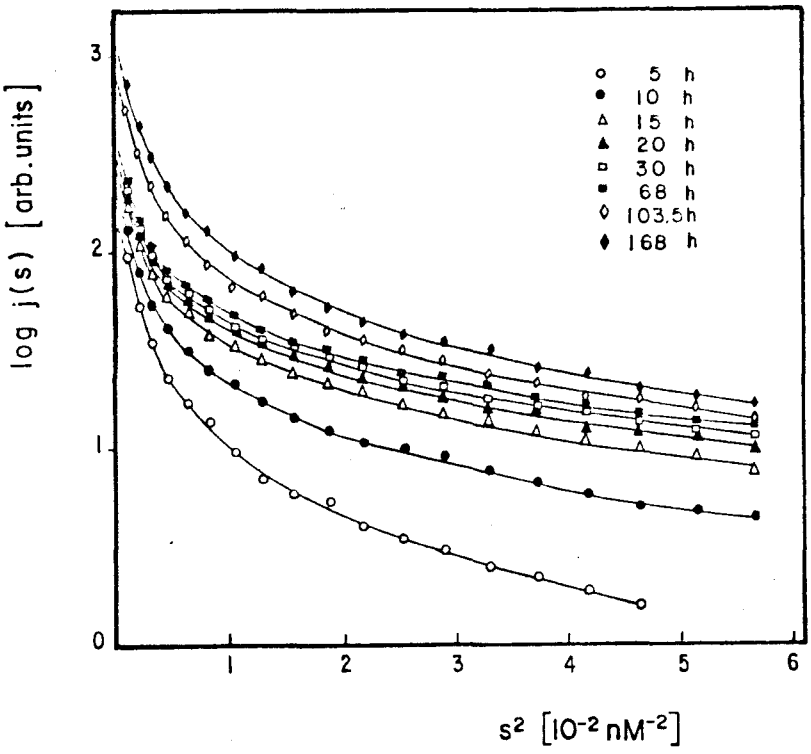
log j(s) [arb.units]
s² [10⁻² nM⁻²]
5 h
10 h
15 h
20 h
30 h
68 h
103.5h
168 h

FIG. 1

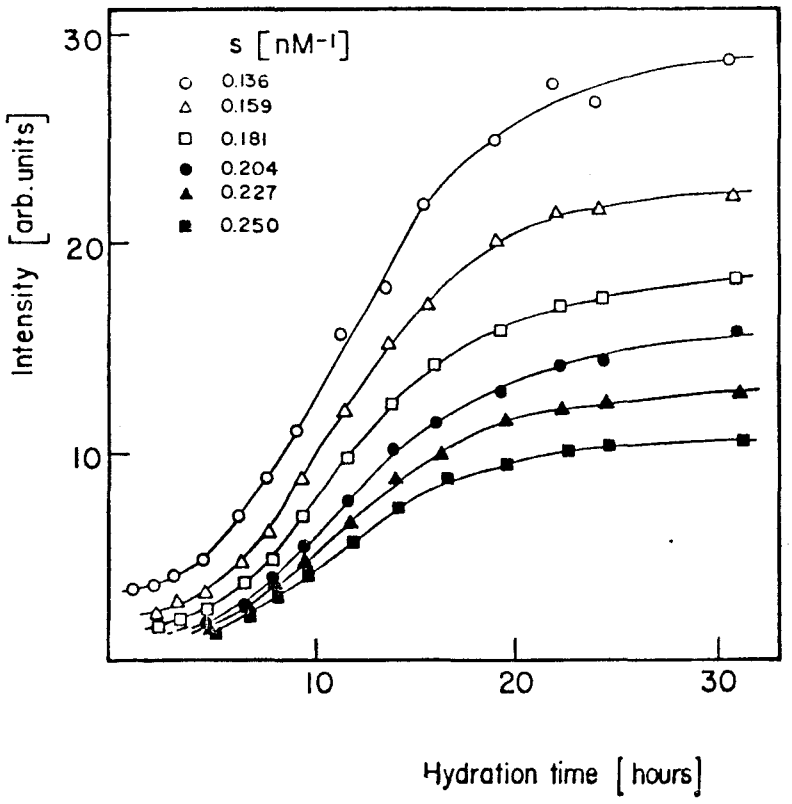
Intensity [arb.units]
Hydration time [hours]
s [nM⁻¹]
0.136
0.159
0.181
0.204
0.227
0.250

FIG. 2

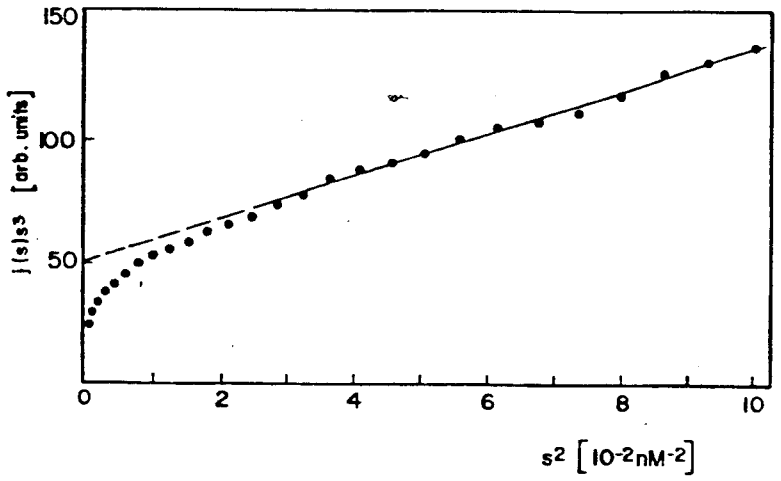
150
100
50
0
2
4
6
8
10
I(s)s³ [arb. units]
s² [10⁻²nM⁻²]

FIG. 3

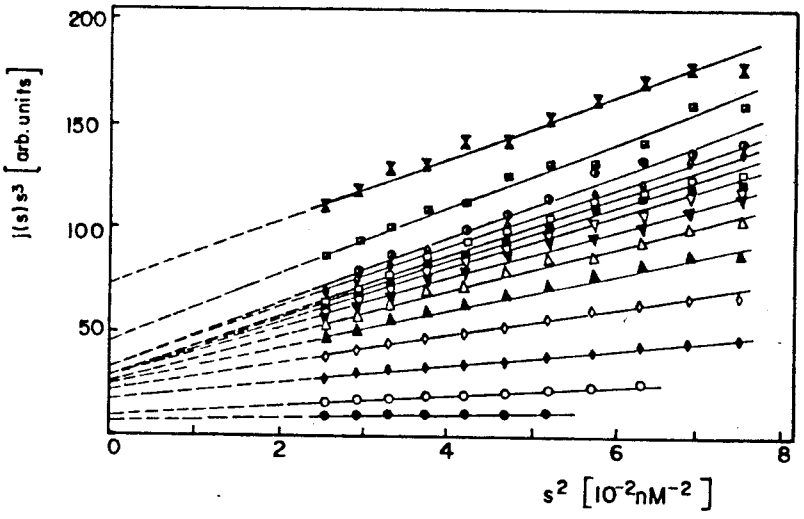
200
150
100
50
0
2
4
6
8
I(s)s³ [arb.units]
s² [10⁻²nM⁻²]

FIG. 4

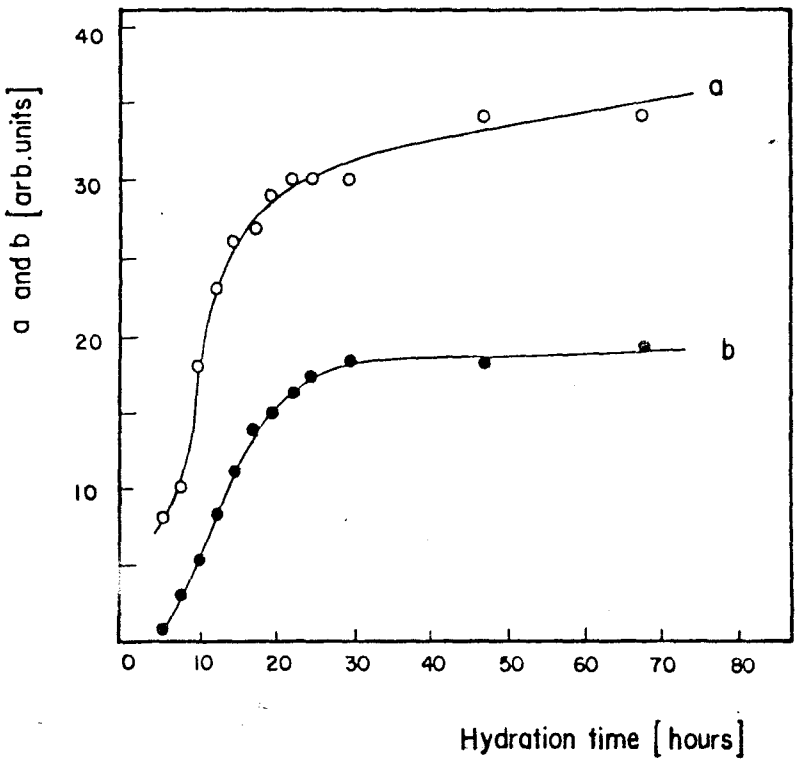
40
30
20
10
a and b [arb.units]
a
b
0
10
20
30
40
50
60
70
80
Hydration time [hours]

FIG. 5

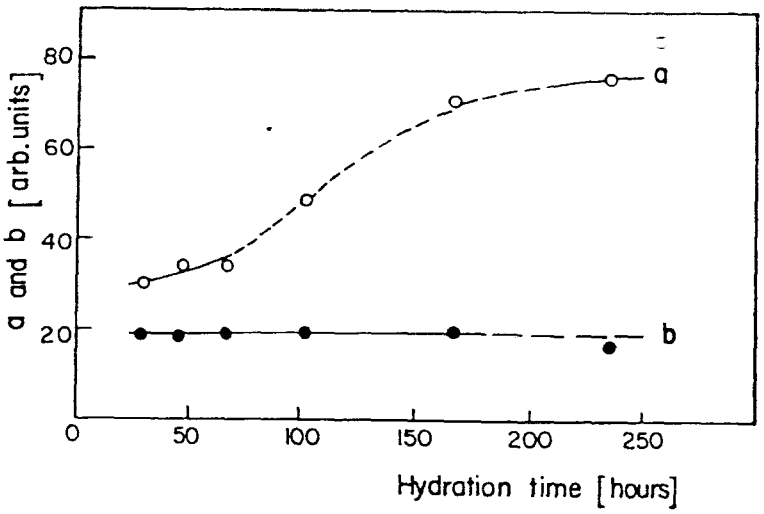
80
60
40
20
a and b [arb.units]
a
b
0
50
100
150
200
250
Hydration time [hours]

FIG. 6